LOW SIDELOBE ANTENNA PATTERNS WITH FAILED ELEMENTS

Steven I. Krich[1], Ian Weiner[1], and Cory J. Prust[2]

[1]MIT – Lincoln Laboratory, Lexington, MA 02420, USA
[2] Milwaukee School of Engineering, Milwaukee, WI 53202, USA

ABSTRACT

Many radar and communication systems utilize phased antenna arrays where it is desirable to maintain low-sidelobes even when one or more individual antenna elements have failed. Traditionally, computing low-sidelobe beamforming with disabled elements requires accurate antenna element patterns. In this paper we present a new algorithm for computing low-sidelobe beamforming that only requires the original beamforming weights that produce low sidelobes when all elements are functioning normally. The algorithm is computationally inexpensive, does not require accurate knowledge of the antenna element patterns, and permits user adjustment of the trade-off between sidelobe level, taper loss, and mainbeam width. Near optimum low sidelobes are demonstrated in several examples.

Index Terms— Array signal processing, beams, linear algebra, phased arrays.

1. INTRODUCTION

For many applications, low spatial sidelobes are required, and it is desirable to maintain these low sidelobes despite the failure of one or more antenna elements. Usually the antenna element patterns are calibrated sufficiently to compute a low spatial sidelobe pattern despite the failure of several elements, as described in References [1-8]. For this paper it is assumed that one knows the low sidelobe beamformers with no failed elements but antenna element patterns are not calibrated well enough to use the referenced techniques. Nothing has been found in the literature for this problem.

Specifically, consider an n element phased array and the following length n vectors. We assume the following are KNOWN and UNKNOWN and all vectors except for $\varepsilon(\theta)$ are unit normed.

UNKNOWN
- $v_t(\theta)$: true steering vector to angle θ
- $\varepsilon(\theta)$: antenna calibration errors, which are large

KNOWN
- $v_a(\theta) = [v_t(\theta) + \varepsilon(\theta)] / |v_t(\theta) + \varepsilon(\theta)|$: assumed steering vector
- $w(\theta)$: low sidelobe beamformer, where the inner product $\langle w(\theta), v_t(\theta + \Delta)\rangle$ is small for Δ in the sidelobe region

The low sidelobe beamformer with failed elements is based exclusively upon the KNOWN vectors and is a linear combination of the $w(\theta)$s. The reader may be wondering how the $w(\theta)s$ could have been determined in the first place. An example will be the subject of a future paper in which an airborne radar's digitally controlled analog beamformer is iteratively adjusted in flight until the sidelobe clutter power is minimized thereby forming a low sidelobe antenna pattern without accurately knowing the individual antenna patterns.

The failed element correction method will be shown to achieve a near optimal solution even if the antenna patterns are accurately known. Thus for some systems, in particular where a rapid recalculation of the beamfomer with failed elements is required, it may be preferable to use this method even if $v_t(\theta)$ is accurately known.

This work is sponsored by the Department of the Air Force under Air Force contract #FA8721-05-C-0002. Opinions, interpretations, conclusions and recommendations are those of the authors and are not necessarily endorsed by the United States Government.

2. FAILED ELEMENT ALGORITHM

Fig. 1 shows a digitally controlled beamformer applied to the $\boldsymbol{n}$ element array to produce a single $\Sigma(\theta)$ beam. If elements are digitized the beamformer is digital otherwise it is analog.

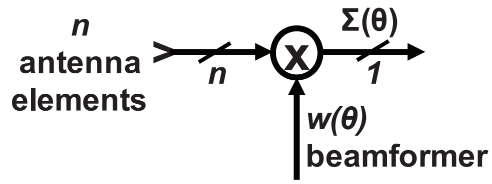

Fig. 1. Beamformer block diagram.

2.1. Beamformer with good antenna calibration

We start by describing a procedure that could be used with good antenna calibration. Let θ be the angle of interest. To the extent permitted by the antenna calibration errors, we could compute a low sidelobe beamformer by letting $R(\theta)$ be a modeled covariance matrix with sidelobe interference. The low sidelobe beamformer with no failed elements is

$$\begin{aligned} \widehat{w}(\theta) &= \mu R(\theta)^{-1} v_a(\theta) \\ R(\theta) &= [\ (1-\gamma) I + \gamma\, M(\theta)\ ] \\ M(\theta) &= \tfrac{1}{L} \textstyle\sum_{|\beta_i - \theta| > \Delta} v_a(\beta_i) v_a(\beta_i)^H \end{aligned} \tag{1}$$

where I is an identity matrix representing the thermal noise, $M(\theta)$ is the modeled interference covariance with no noise, γ controls the mixture of modeled interference to thermal noise, 2Δ is the width of the mainlobe, L is the number of terms in the sum, μ is a normalizing scale factor, and H is Hermitian transpose.

With failed elements the above equations can be modified to delete the rows and columns of $R(\theta)$ and $v_a(\theta)$ corresponding to the location of the failed elements. However, with or without failed elements, the procedure will fail to achieve low sidelobes if the antenna calibration errors are large. The next section describes how to overcome the antenna calibration limitations.

2.2. Beamformer with constraints

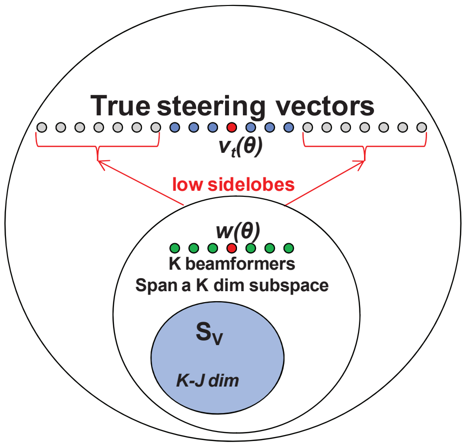

Fig. 2. Beamformer properties in an n dimensional space.

Here we constrain the above solution to a reduced dimension vector space in order to overcome the calibration errors. Let W_K be a matrix whose columns are K low sidelobe beamformers surrounding the direction θ of interest. These should be closely spaced (less than a beamwidth) and preferably include $w(\theta)$ as a column. As illustrated in Fig. 2 representing an n dimensional vector space, all of these beamformers have low sidelobes.

We constrain the solution to this vector space as follows. Let $J < K$ be the number of failed elements and $D = [d_1, d_2, \ldots, d_J]^T$ be a vector for the locations of the failed elements. Within the space spanned by W_K is a subspace S_V of dimension $K - J$ where all vectors in S_V have a 0 at the locations of the failed elements. We compute this subspace as follows. Using MATLAB notation, $W_K(D,:)$ is a $J \times K$ matrix of only the rows of W_K with failed elements. The $K \times J$ matrix $null(W_K(D,:))$ is an orthonormal basis for the null space of $W_K(D,:)$ obtained from the singular value decomposition. That is, $W_K(D,:)[null(W_K(D,:))]$ is a $J \times (K - J)$ matrix of 0s and thus

$$V = W_K[null(W_K(D,:))] \quad (2)$$

is an $n \times (K - J)$ matrix with 0s along the rows corresponding to the location of the J failed elements. The subspace spanned by the columns of V is S_V. We constrain the solution to S_V, thereby modifying (1) as follows

$$\begin{aligned}\hat{w}(\theta) &= \mu V[V^H R(\theta) V]^{-1} V^H v_a(\theta) \quad (3)\\ &= \mu V[(1-\gamma)V^H V + \gamma V^H M(\theta) V]^{-1} V^H v_a(\theta).\end{aligned}$$

If $M(\theta)$ is approximately known, but not necessarily with perfect accuracy, then it may be used here. However, for the cases of interest we will assume that the calibration errors are too large to provide a good estimate of $M(\theta)$, and instead we will approximate $V^H M(\theta) V = \alpha I$ where α is the average sidelobe level achieved by the beamforms in W_K. It can be mathematically shown, but is beyond the scope of this paper, that this is a good approximation for this application and enables an accurate estimate of the achieved sidelobes when choosing parameters in the next section. Furthermore the examples verify this. Thus

$$\hat{w}(\theta) = \mu V[(1-\gamma)V^H V + \gamma\alpha I]^{-1} V^H v_a(\theta) \quad (4)$$

where in this transformed space $V^H V$ is the correlated thermal noise and αI is the interference covariance estimate. Since μ is a factor making $\hat{w}(\theta)$ unit norm, we can drop α and replace μ and γ by $\tilde{\mu}$ and $\tilde{\gamma}$ where $\tilde{\mu}$ is a normalizing factor and $0 \leq \tilde{\gamma} \leq 1$.

$$\hat{w}(\theta) = \tilde{\mu} V[(1-\tilde{\gamma})V^H V + \tilde{\gamma} I]^{-1} V^H v_a(\theta)\,. \quad (5)$$

In choosing parameters K and $\tilde{\gamma}$ it is useful to have an estimate for the change in the taper loss and average sidelobes. Unless the calibration errors are extremely large a good taper loss estimate in dB is $TL(\hat{w}) = 10log_{10}|\hat{w}(\theta)^H v_a(\theta)|^2 \leq 0$ where $\hat{w}(\theta)$ and $v_a(\theta)$ are unit normed. To estimate the average sidelobes we can rewrite $\hat{w}(\theta) = Vc$ where c is the $K - J$ vector of coefficients for combining the columns of V. Recalling that α is the average sidelobe level estimate with no failed elements we can estimate the change in the average sidelobe as

$$\begin{aligned}\Delta \mathrm{SL}_{\mathrm{est}}(\hat{w}(\theta)) &= 10log_{10}[\hat{w}(\theta)^{\mathrm{H}}\, \mathrm{M}(\theta)\hat{w}(\theta)/\alpha]\\ &= 10log_{10}[c^H V^H M(\theta) V c/\alpha] \quad (6)\\ &= 10log_{10}|c|^2\,.\end{aligned}$$

2.3. Choosing parameters K and $\tilde{\gamma}$

As before, $\tilde{\gamma}$ in (5) controls the mixture of modeled interference to thermal noise. Constrained by K to the chosen vector space, $\tilde{\gamma} = 0$ is the matched filter and $\tilde{\gamma} > 0$ is the colored noise matched filter to reduce sidelobes. Stated differently for $\tilde{\gamma} = 0$ this is a projection onto the space spanned by the columns of V. Thus $\tilde{\gamma} = 0$ has the best taper loss but the highest sidelobes. As $\tilde{\gamma}$ increases, the taper loss monotonically degrades and the sidelobes improve. $\tilde{\gamma} > 0$ has the effect of regularizing the matrix $V^H V$ by reducing the contribution the eigenvectors corresponding to the small eigenvalues of $V^H V$. These monotonicity properties are very useful for the procedure.

The procedure is flow charted in Fig. 3 in which values for K and $\tilde{\gamma}$ are found such that $\Delta SL_{est}(\hat{w}) = \Delta SL_{goal}$ and the taper loss, $TL(\hat{w})$, is lower bounded by $\mathrm{TL}_{\mathrm{bound}}$. (Note: $\Delta SL_{goal} = 0$ means unchanged sidelobes and $TL(\hat{w})$ is negative.) Finding $\tilde{\gamma}$ in the interval [0,1] is simplified by the monotonicity discussed above for the function in (5).

For unrealistic goals, K may continue to increase to an unacceptably large value and a solution may not be found. In this case the goals should be reset and the procedure repeated.

The procedure is easily modified to have $TL(\hat{w}) = TL_{goal}$ and $\Delta SL_{est}(\hat{w}) \leq \Delta SL_{bound}$.

3. EXAMPLES

Near optimum performance has been demonstrated with one- and two-dimensional arrays as illustrated by these examples.

The authors feel it is important that the validity of algorithms be tested under real-world conditions. Specifically, we test the procedure using a perfect uniform linear array as the assumed steering vectors, $v_a(\theta)$, but the true steering vectors, $v_t(\theta)$, having small perturbations from the perfect uniform linear array. These perturbations, $\varepsilon(\theta)$, are independent from element to element, and change slowly with angle. The calibrations errors

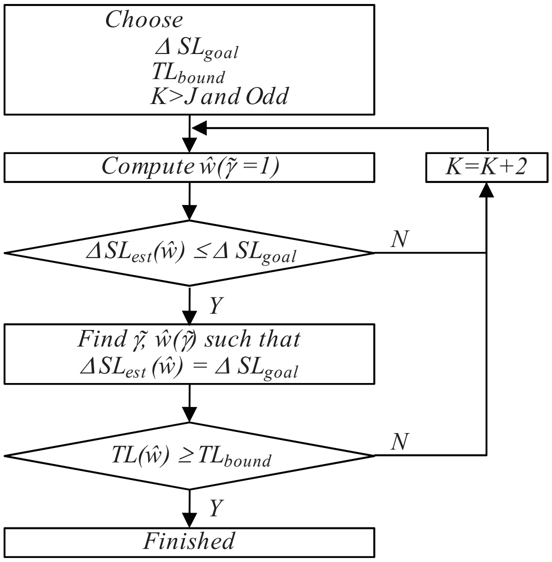

Fig. 3. Procedure for choosing parameters.

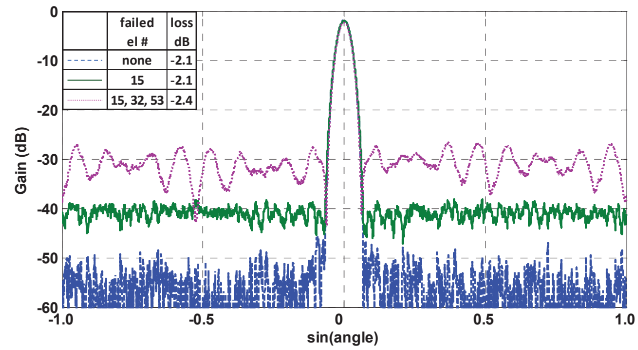

Fig. 4. Uncorrected antenna patterns with failed elements in a 64 element linear array.

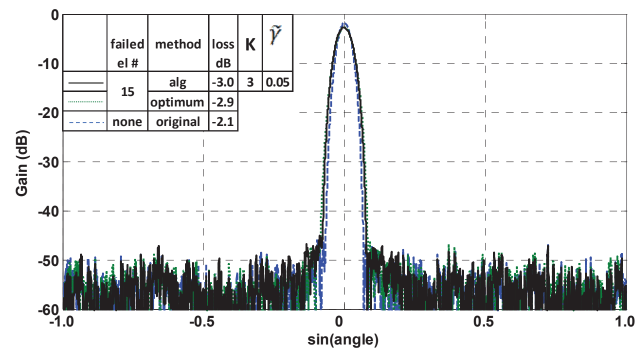

Fig. 5. Corrected antenna patterns with failed element 15.

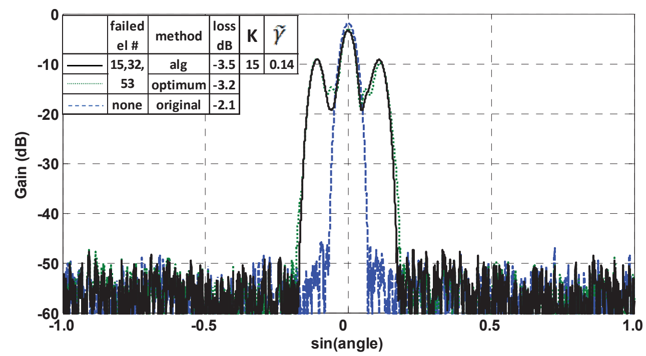

Fig. 6. Corrected antenna patterns with failed elements 15, 32, and 53.

limit the achievable beamformer sidelobes based solely upon the assumed array calibration to -30 dB with or without failed elements. Even with perfect array calibration knowledge, the angle dependent element pattern differences limit the best sidelobes to about -51 dB. However, we will assume that the beamforming weight vectors, $w(\theta)$, to achieve -50 dB sidelobes with no failed elements are available. The beams in W_K are spaced by a half beamwidth.

Fig. 4 shows the antenna patterns with various combinations of failed elements [none], [15], [15,32,53] without any correction in a 64 element linear array. The taper loss numbers are relative to the true steering vectors, $v_t(\theta)$.

Fig. 5 shows the resulting corrected patterns with element [15] failure to yield unchanged sidelobes, $\Delta SL_{goal} = 0\,dB$ and $TL_{bound} = -3.5\,dB$. The relevant parameters K, $\tilde{\gamma}$, and taper loss are indicated. Notice the taper loss is better than the bound. In order to evaluate the performance of the correction algorithm, we include a comparison with an optimum approach using (1), $v_a(\theta) = v_t(\theta)$ and γ selected to maintain the sidelobe levels at $-50\,dB$ and 2Δ chosen to be the angular width of the K beams in the algorithm. Notice that the algorithm and optimum patterns virtually overlay with taper losses within a tenth of a dB. All patterns have the same sidelobe levels but the corrected patterns have a slightly wider mainlobe.

Fig. 6 repeats the previous example with three failed elements, [15,32,53], and similar agreement is achieved between the algorithm and optimum. The high first sidelobe is primarily due to deleting an element in the middle of the array.

Figs. 7 and 8 illustrate a two-dimensional 16 x 16 element array. Again the calibration errors are independent from element to element and change slowly with angle. Fig. 7 illustrates the pattern with no failed elements and Fig. 8 after correction with two failed elements [4,8] and [8,12], again using $\Delta SL_{goal} = 0\,dB$ and $TL_{bound} = -3.5\,dB$. In the 2D case neighboring beams are taken in groupings that extend symmetrically in both $\sin(az)$ and $\sin(el)$ space. The choice $K = 13$ used here corresponds to a diamond-shaped grouping of beams centered around the beam to be corrected.

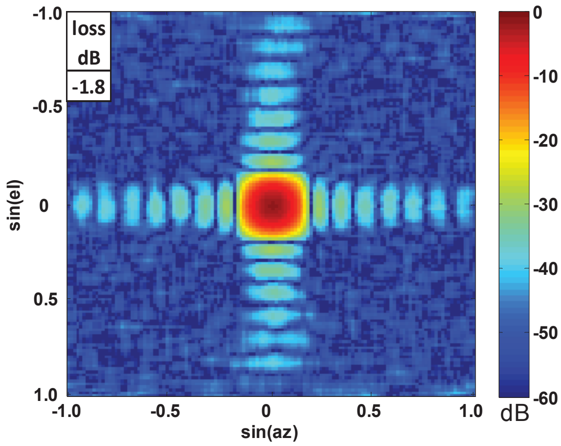

Fig. 7. Low sidelobe pattern for a 16 x 16 array.

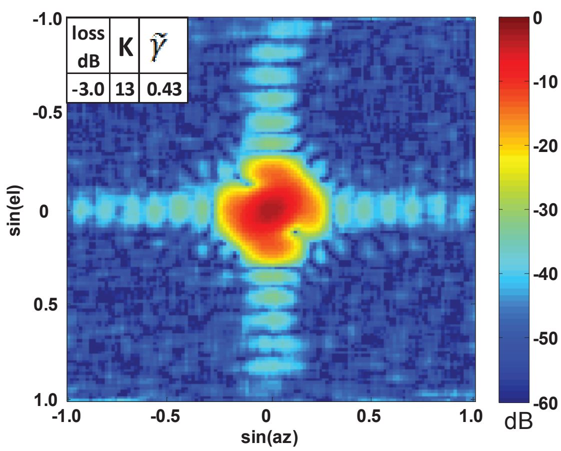

Fig. 8. Corrected pattern with two failed elements [4,8] and [8,12].

4. PULSE-DOPPLER RADAR APPLICATION

As is frequently the case, techniques developed in either the spatial or the temporal domain frequently find application in the other domain. Consider a pulse-Doppler radar in which one or more pulses are severely interfered with but low Doppler sidelobes are needed with these pulses dropped. Mathematically, the missing pulses replace the failed elements, and the Doppler filters replace the low sidelobe beamformers. The techniques in this paper offer a rapid and predicable outcome for taper losses and Doppler sidelobe level. Since here calibration is likely not to be an issue, it may be preferable to use (3) instead of the approximation in (5) for the covariance matrix. Furthermore, since calibration is not an issue, the techniques in the literature are also applicable but may be more computationally intense with little added benefit.

Similarly temporal samples in the range domain may be interfered with and low range sidelobes are needed even with these dropped samples. Mathematically the pulse compression filter replaces the low sidelobe beamformers.

5. SUMMARY

Given that the original low-sidelobe beamformers are available but antenna calibration data to the corresponding level of accuracy are not, a natural approach is to form the corrected beams as linear combinations of the original beams. We observed that linear combinations of these beams had a 0 at the location of the failed elements and we constrained the solution to this vector space, S_V. To choose the parameters K and $\tilde{\gamma}$ we derived an approximation for the change in sidelobe level as $\|c\|^2$. Since we have measures for the change in sidelobe level, taper loss, and mainbeam region, we can find an optimal set of parameters to satisfy these conditions. We have thus demonstrated a robust method for calculating a low sidelobe beamformer with failed elements where we can control the achieved sidelobe levels, the taper loss, or the width of the mainbeam region.

The approach is also applicable to forming beams with no failed elements to reduce taper losses by raising the sidelobes. Also discussed was the application of the algorithm in pulse-Doppler radars for missing pulses or missing range samples with the goal of maintaining low Doppler sidelobes or range sidelobes.

The method has been shown to be near optimal and thus may find application even for systems with good antenna calibration.

REFERENCES

[1] W. P. Keizer, H. Stark, "Element failure correction for a large monopulse phased array antenna with active amplitude weighting," IEEE Trans. Antennas and Propagation, vol. 55, No. 8, pp. 2211-2218, August 2007.

[2] M. H. Er, "Array pattern synthesis in the presence of element failure," Proceeding of the ISAP '92, Sapporo, Japan, pp. 9–12, 1992.

[3] K. M. Lee, R. Chu, S. Liu, "A built-in performance monitoring/fault isolation and correction (PM/FIC) system for active phased array antennas," *IEEE Antennas and Propagation Society International Symposium* 1993, pp. 206–9, vol. 1.

[4] S. Liu, "A fault correction technique for phased array antennas," *IEEE Antennas and Propagation Society International Symposium 1992 Digest.* Publication Date: URSI Radio Science Meeting and Nuclear EMP Meeting, 1612–15, vol. 3, 1992.

[5] T. J. Peters, "A conjugate gradient-based algorithm to minimize the sidelobe level of planar arrays with element failures," IEEE Trans. Antennas and Propagation, vol. 39, No. 10, pp. 1497–1504, October 1991.

[6] P. J. Wright and D. Brandwood, "Re-optimisation of linear and planar arrays with failed elements," Ninth International Conference on Antennas and Propagation, pp. 81–84, vol. 1, 1995.

[7] S. H. Zainud-Deen, M. Ibrahem, H. Sarshar, and S. Ibrahem, "Array failure correction with orthogonal method," 21st National Radio Conference (NRSC2004) (NTI), March 2004.

[8] Y. Yang, "Design of self-healing arrays using vector-space projections," IEEE Trans. Antennas and Propagation, Vol. 49, No. 4, pp. 526-534, April 2001.